Theoret. chim. Acta (Berl.) 24, 89—98 (1972)

SCC–EH–MO Calculations on the Bonding and Electric Field Gradient in Oxyhaemoglobin and Other Haem Derivatives

MARGARET P. HALTON
Chemistry Department, Victoria University of Wellington, New Zealand

Received September 27, 1971

SCC–EH–MO theory satisfactorily accounts for the sign and relative magnitude of the electric field gradient at the nucleus in several haem derivatives. The bonding in oxyhaemoglobin and some iron(III) porphyrins is discussed and a theory for the stability of oxyhaemoglobin is examined.

Die SCC–EH–MO Theorie gibt für einige Häm-Derivate zufriedenstellend die Verhältnisse bezüglich Vorzeichen und relativer Stärke des elektrischen Feldgradienten beim Kern wieder. Die Bindungsverhältnisse in Oxyhämoglobin und einigen Eisen(III)porphyrinen werden diskutiert, und eine Theorie für die Stabilität von Oxyhämoglobin wird geprüft.

Introduction

Bonding in iron porphyrins continues to be a subject of much interest because of their well known biological significance. A variety of theoretical methods have been employed but several experimental features have not yet been explained. In particular, for haemoglobin derivatives, the Mössbauer spectra have not been fully accounted for, while the unusual stability of the oxygen binding in oxyhaemoglobin has been well characterised [1] but not completely understood. We report now the application of a model system, based on SCC–EH–MO's (Self Consistent Charge Extended Hückel Molecular Orbitals), to examine the quadrupole splitting in the Mössbauer spectrum and the nature of the bonding in a number of iron porphyrin (haem) derivatives.

Method

The formalism of Extended Hückel theory (EHT) is well known [2], and only the important features included in this paper. Diagonal elements, H_{ii}, of the $\boldsymbol{H}$ matrix were taken from valence state ionisation energies (VSIE's) which have been obtained from spectral data. Zerner and Gouterman's values [3] were used for the iron, and Hinze and Jaffé's [4] for all other atoms. The off-diagonal terms, H_{ij}, were constructed from the Wolfsberg-Helmholtz relation [5].

a) The Model

An all valence orbital calculation of the complete iron porphyrin system (Fig. 1) involves more than 125 orbitals, and the computing facilities available to us could not handle such a large basis set. Group theoretical methods could not

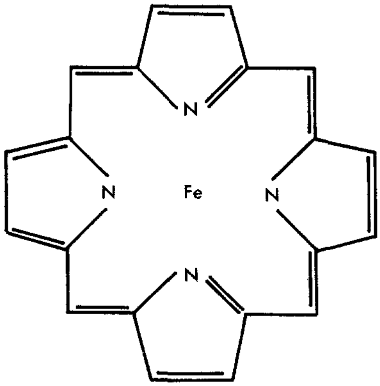

Fig. 1. Iron porphyrin

Table 1. Systems studied

System	Simulated species[a]	Spin	Sixth ligand	Ligand orbitals	Details
1	Hb	2	—	—	—
2	HbO_2	0	O_2	all 2*s*, 2*p*	$A, a = 0°$
3	HbO_2	0	O_2	all 2*s*, 2*p*	$A, a = 60°$
4	HbO_2	0	O_2	all 2*s*, 2*p*	$B, b = 0°$
5	HbO_2	0	O_2	all 2*s*, 2*p*	$B, b = 60°$
6	HiH_2O	5/2	H_2O	2*s*, 2*p*, 1*s*	acid form
7	HiOH	5/2	O^-	2*s*	basic form
8	HiOH	3/2	O^-	2*s*	basic form
9	HiOH	1/2	O^-	2*s*	basic form low temperature
10	HiCl	5/2	Cl^-	3*s*	in pyridine solution
11	HbCO	0	C	(*sp*)	

[a] Hb denotes iron(II) haemoglobin; Hi denotes iron(III) haemoglobin.

be used because we are interested in some asymmetric geometries of the oxygenated system. Furthermore, since computing time increases rapidly with the size of the basis set, we required a model system which minimised the matrix order but which still effectively simulated the iron in the porphyrin environment.

Because the electron distribution around the iron itself is of prime interest in this work, all valence orbitals (3*d*, 4*s*, 4*p*) of the iron were included, but only the nitrogen orbitals of the porphyrin ring. Each porphyrin nitrogen was represented by a pi orbital in the z direction and a trigonal hybrid (sp^2) orbital in the xy plane (plane of the porphyrin). An sp^2 orbital was used so that the geometry of the porphyrin sigma system was imposed upon the model. Recent workers have shown [6] that sp^2 hybridisation is an adequate picture of the nitrogen orbital in an analogous copper complex. The fifth ligand was represented by a single neutral nitrogen sp^2 hybrid orbital, since the protein of haemoglobin co-ordinates to the iron through an imidazole [7]. The orbitals employed for the sixth ligand are given in Table 1. The overlap integrals of Ohno *et al.* [8] were used for the iron-nitrogen bonds and all other overlap integrals were calculated from Slater atomic orbitals [9]. Zerner *et al.* [10] have examined the effects of non-planar metal porphyrin and their results showed little difference in orbital populations between planar and non-planar systems. Consequently we assumed the iron to lie in the porphyrin plane. Errors arising from the use of a limited basis set are constant for all haem systems studied and therefore a significant discussion of experimental trends and bonding of the iron itself can be made.

Iterative EH calculations were performed using the self consistent charge (SCC) procedure of Zerner and Gouterman [3]. Because EHT does not include electron repulsion terms, the number of unpaired electrons was imposed upon the calculation. All computations were performed on an Elliott 503 computer, using modifications of Bailey's programs [11].

b) Choice of Systems

Haem derivatives were selected for study which had available Mössbauer data and these systems are listed in Table 1. The bonding in oxyhaemoglobin has been the subject of much controversy but two main cases have been proposed, the Pauling [12] and Griffith [13] models (see Fig. 2, $A, a = 60°$ and $B, b = 0°$ respectively). A systematic study of several geometrical arrangements has been made [14] and two were calculated to be particularly stable (in Fig. 2, $A, a = 60°$ and $B, b = 60°$). These two geometries were studied using the SCC model reported here, together with the extreme cases ($A, a = 0°$ and $B, b = 0°$). The bond lengths used were: iron-oxygen = 2.1 Å, oxygen-oxygen = 1.48 Å [14]. Reduced haemoglobin has no ligand in the sixth position [7] and was simulated by system 1 (see Table 1). The acid form of iron(III) haemoglobin contains water in the fifth position and is high-spin [15], but the basic form, with hydroxide in the sixth position, has unusual spin behaviour. At low temperatures, $S = 1/2$ appears to be correct [16] but at room temperature the magnetic moment corresponds to a spin of 3/2 and has been ascribed to an equilibrium of the high-spin ($S = 5/2$) and low-spin forms [17]. Therefore, we examined the three possible spin states ($S = 1/2, 3/2, 5/2$). System 10, in Table 1, was assumed to simulate chloro-iron(III) protoporphyrin IX in pyridine solution, since a nitrogen sp^2 orbital was used in the fifth position for every system studied. Since the iron itself is of prime interest for systems 5–11, a limited set of basis orbitals was used for several of these systems in order to minimise computing time. Because the Mössbauer results were found to be successful, this assumption was not modified. Whenever a single orbital was employed for the axial ligands, a fixed charge for that ligand was assumed in the iterative procedure.

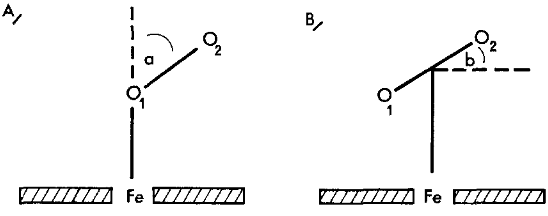

Fig. 2. Geometries of oxygenated iron porphyrin

c) Calculation of Electric Field Gradient

Mössbauer data are particularly useful in testing the theoretical model of this work since EHT is suitable only for ground state properties and the Mössbauer spectrum pertains to ground state iron alone. The electric field gradient, EFG, at the nucleus is determined from the MO coefficients [18]:

$$V_{zz} = -e\Sigma\langle\psi_i|3\cos^2\theta_i - 1|\psi_i\rangle\, N_i\langle r^{-3}\rangle \tag{1}$$

and

$$V_{xx} - V_{yy} = -e\Sigma\langle\psi_i|3(x_i^2 - y_i^2)/r_i^2|\psi_i\rangle\, N_i\langle r^{-3}\rangle \tag{2}$$

where N_i is the number of electrons in MO ψ_i, and $(-e)$ the electron charge. (The cross terms of the EFG tensor V are neglected). The observed quadrupole splitting ΔE_Q is proportional to the EFG, such that

$$\Delta E_Q \propto V_{zz}(1 + \eta^2/3)^{\frac{1}{2}} \tag{3}$$

where

$$\eta = (V_{xx} - V_{yy})/V_{zz}\,.$$

For convenience, Eqs. (1)–(3) were simplified by introducing a parameter B which was directly proportional to ΔE_Q, and the constants e and $\langle r^{-3}\rangle$ incorporated into the proportionality constant. The sign of B was then the predicted sign of the EFG, and the sign convention adopted was such that a positive EFG implied that the nuclear excited 3/2 state was higher in energy than the nuclear excited 1/2 state. Thus, for zero η B is given by:

$$B = [N_{x^2-y^2} + N_{xy} - (N_{xz} + N_{yz})/2 - N_{z^2}]\, 4/7 + [N_x + N_y - 2N_z]\, 2/5 \tag{4}$$

where N_j is the gross atomic population for basis orbital j, and j covers all $3d$ and $4p$ iron orbitals. The expression for B when $\eta \neq 0$ follows readily. There are two major assumptions in this formulation of B; first that $\langle r^{-3}\rangle$ is the same for both $3d$ and $4p$ orbitals, and second, that the use of GAP values, which are appropriate for $3d$, are also appropriate for $4p$. However, errors arising from these assumptions were found to cancel for the systems studied here [19].

Results and Discussion

In the following discussions, the MO's are often referred to as a particular atomic orbital, for convenience. This implies that the MO is predominantly that atomic orbital in character and not necessarily pure atomic orbital. In fact, only the $3d_{xy}$ iron orbital is ever found to be a pure atomic orbital in these systems. Only those results pertinent to the discussion are recorded, and these in the appropriate sections below.

a) Electric Field Gradient

The gross atomic populations (GAP) for the iron orbitals in each of the systems 1–11 are listed in Table 2, and the consequent B values are given in Table 3. The experimental sign of the EFG is known for the molecules simulated by systems 1–6 and 10, and in each case experiment and theory agree. Because of this agreement for all known cases, we assumed that the sign of B

Table 2. Iron orbital populations

System	1	2	3	4	5	6	7	8	9	10	11
$4s$	0.330	0.312	0.346	0.258	0.367	0.317	0.404	0.448	0.473	0.434	0.323
$4p_x$	0.071	0.104	0.108	0.091	0.108	0.077	0.076	0.094	0.106	0.078	0.073
$4p_y$	0.071	0.104	0.102	0.105	0.106	0.089	0.076	0.094	0.106	0.078	0.073
$4p_z$	0.221	0.253	0.326	0.148	0.319	0.267	0.255	0.307	0.303	0.281	0.215
$3d_{xy}$	2.000	2.000	2.000	2.000	2.000	2.000	2.000	2.000	2.000	2.000	2.000
$3d_{yz}$	1.433	2.000	2.000	2.000	1.876	1.531	1.500	1.708	1.896	1.502	2.000
$3d_{xz}$	1.433	2.000	1.988	1.933	1.958	1.520	1.500	1.708	1.896	1.502	2.000
$3d_{z^2}$	0.917	0.452	0.796	0.297	0.938	0.950	1.023	1.069	0.381	1.056	0.312
$3d_{x^2-y^2}$	1.117	0.289	0.306	0.255	0.304	1.131	1.124	0.303	0.341	1.127	0.241
Fe chge	0.407+	0.486+	0.028+	0.913+	0.024+	0.120+	0.042+	0.269+	0.498+	0.058−	0.763+

Table 3. Theoretical and experimental EFG

System	Molecule	B	ΔE_Q mm/sec	Ref.
1	Hb	+0.318	+2.40	[20]
2	HbO_2	−0.212	−2.25	[21]
3	HbO_2	−0.455	−2.25	[21]
4	HbO_2	−0.015	−2.25	[21]
5	HbO_2	−0.486	−2.25	[21]
6	HiH_2O	+0.228	+2.00	[21]
7	HiOH	+0.220	1.57	[21]
8	HiOH	−0.441	1.90	[21]
9	HiOH	−0.196	0.98	[20]
10	HiCl	+0.163	+0.78	[20]
11	HbCO	−0.155	0.36	[21]

corresponded to the sign of the EFG in every system. We plotted the experimental quadrupole splitting (see Table 3) against B for the systems 1, 6, 9–11 and obtained an excellent linear correlation (Fig. 3). Only the low-spin case for HiOH ($S = 1/2$) was included in this plot since the higher spin states correspond

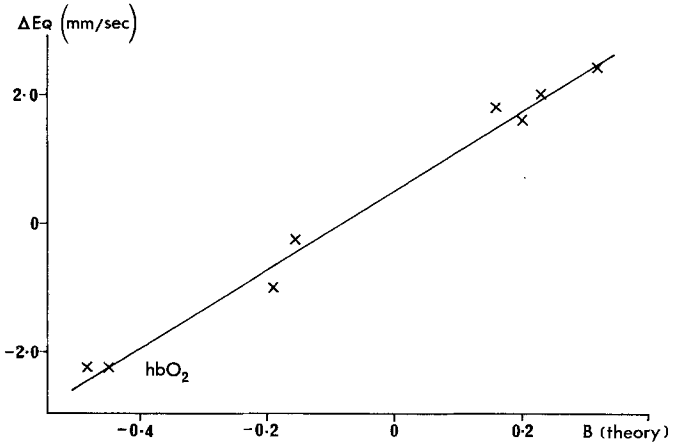

Fig. 3. Plot of experimental quadrupole splitting against theoretical electric field gradient parameter, B

to higher temperatures and MO calculations are most pertinent at very low temperatures. This species is discussed further below. Fig. 3 also shows the position of systems 3 and 5 but the oxygenated cases are discussed separately.

The satisfactory correlation demonstrates the success of our model in spite of its approximations and the inherent assumptions of SCC–EHT. Hence, our consequent deductions about the systems studied are justified, provided the limitations of the model are remembered. Our correlation plot is much better than that achieved by other workers [22] who used similar calculations, and reasons for this will become clear in the following discussions.

b) High-Spin Iron(III) Porphyrins

The two high-spin iron(III) derivatives studied, systems 6 and 11, have led to the first successful prediction of the sign of their EFG. Several workers [22, 23] have examined these species using the MO calculations of Zerner *et al.* [10] but all have predicted negative EFG values, contrary to experiment [23]. The successful prediction in our work arises from the assumption of a new ground state. We found, as have other workers [10], that the relative energies of the highest occupied MO's are:

$$xy < a_1 < xz \sim yz < z^2 < x^2 - y^2$$

where a_1 denotes the highest occupied MO of porphyrin pi orbitals, assuming C_{2v} symmetry. This ordering of the energy levels leads to the $^6A_2(d^6)$ configuration:

$$(xy)^2\,(a_1)^1\,(xz)^1\,(yz)^1\,(z^2)^1\,(x^2-y^2)^1$$

which we adopted in the SCC procedure but Zerner *et al.* [10] insisted upon the $^6A_1(d^5)$ configuration

$$(xy)^1\,(a_1)^2\,(xz)^1\,(yz)^1\,(z^2)^1\,(x^2-y^2)^1$$

in their calculations. The multiplicity of both configurations correspond to the magnetic susceptibility data [15] but since the Mössbauer spectrum pertains to the iron itself, not the entire system, the EFG is a more appropriate experimental quantity to use to distinguish between the alternative configurations. The $^6A_1$ state leads to a negative EFG [22] contrary to experiment [23], while the $^6A_2$ state not only predicts correctly a positive EFG but also accounts for the unusually large observed value of the quadrupole splitting. Furthermore, esr data for these derivatives have been explained by assuming a large asymmetry in the iron environment [24]. Such asymmetry is unusual for high-spin d^5 species but characteristic of high-spin d^6. Our calculations refer to low temperatures and a thermal equilibrium between the $^6A_1$ and $^6A_2$ states may exist at room temperature. Experimental properties such as isomer shifts and absorption spectra cannot be examined with SCC–EHT because of the inherent approximations. However, a detailed theoretical study of these properties will be necessary before the proposed $^6A_2$ ground state can be confirmed.

c) Iron(III) Haemoglobin Hydroxide

The spin state of the hydroxide derivative has not been well established. However, at room temperature the magnetic susceptibility corresponds to a spin of 3/2 [17] while at 5° K esr data indicates a spin of 1/2 [16]. Mössbauer spectra have been observed [21] at 4° K, 77° K, and 195° K, and if Blume's [25] arguments are followed, the EFG is negative at 4° K but positive at 77° K and 195° K. We predict a negative EFG for the $S=1/2$ case (system 9), positive EFG for $S=5/2$ (system 7), and negative EFG for $S=3/2$ (system 8). The magnitude of the calculated EFG parameter, B, follows the correlation curve in Fig. 3 for all three systems, and hence only the sign of the EFG for the $S=3/2$ case is unexplained. A detailed experimental study of magnetic susceptibilities over a wide temperature range and a careful examination of the 3/2 state and possible equilibria between 5/2 and 1/2 will be required before the hydroxide case is fully understood.

d) Oxyhaemoglobin

Considerable difficulty was encountered with systems 2–5 (the oxygenated species) in positioning the 3*d* orbitals and achieving satisfactory convergence. This arose because the oxygen 2*p* orbitals were lower in energy than the iron 3*d* orbitals, so that electrons were assigned to the oxygen orbitals at the expense of those of the iron. In effect the MO calculations were predicting that oxidation would occur, and this is observed generally for iron(II) porphyrins. These theoretical difficulties were overcome by adding two electrons to the system; because oxyhaemoglobin is diamagnetic [15] any extra electrons must be added in pairs. Our theoretical model can be compared with that of Zerner *et al.* [10]. These workers examined two geometries only, corresponding to $A, a=0°$ and $B, b=0°$ in Fig. 2, and did not add two extra electrons. For the linear case ($A, a=0°$) they found that the oxygen 2*p* orbitals were much lower in energy than the iron 3*d*, as we found, and concluded that oxidation would occur. Their case corresponding to $B, b=0°$, converged satisfactorily but, because all of the porphyrin valence orbitals had been included, the porphyrin was able to compensate for the electron loss to the oxygen orbitals. Of all the systems studied by Zerner *et al.*, only this case led to a positive charge on the porphyrin nitrogens. Furthermore, Zerner *et al.*'s MO's lead to a positive EFG [22], contrary to experiment [21]. Our MO's determined with the two extra electrons, lead to a negative EFG, in agreement with experiment (see Table 3).

In view of these results, and the demonstrated success of our theoretical model, a theory which accounts for the unusual stability of oxyhaemoglobin, and oxymyoglobin, has been proposed [19]: oxidation of iron(II) porphyrin will occur unless two electrons are added to the oxygenated iron. Since haemoglobin is an oxygen carrier and not part of an enzyme system, the protein is presumed to provide the electrons through the fifth ligand and the delocalised pi orbitals of the porphyrin. Indirect experimental evidence is available from studies of oxygen binding in some cobalt complexes and reconstituted haems and haemoglobins. Caughey *et al.* [26] have shown that an increase in the pi electron donation to the metal enhances oxygen binding and this can be understood from our pro-

Table 4. Results for oxygenated systems

System[a]	2	3	4	5
Chge O^1	−0.830	−0.618	−0.901	−0.688
Chge O^2	−0.930	−0.751	−0.934	−0.816
Chge O^1+O^2	−1.760	−1.369	−1.835	−1.504
NOP O^1	0.261	0.294	0.185	0.280
NOP O^2	0.142	0.157	0.182	0.159
NOP O^1+O^2	0.403	0.451	0.367	0.439

[a] O^1 refers to oxygen closest to the iron, O^2 to distal oxygen.

posed theory: the electrons lost to the oxygen are from the metal d_π orbitals so that any factor which increases the pi electron donation will increase the stability of the metal-oxygen system. Several workers [27] have established that an increase in the basicity of the fifth ligand in model systems leads to an increased oxygen affinity, and this correlates with our proposed requirement of electron transfer to the iron to compensate for the loss to the oxygen.

There are two main features of this theory of two electron transfer: first, the iron exists as a d^6 species in oxyhaemoglobin, and second, the oxygen molecule exists as an oxyanion (see Table 4). These features can be compared with the suggestions of other workers. Weiss [28] proposed that the electron distribution in oxyhaemoglobin corresponds to Fe(III).O_2^-. We have calculated a large negative charge on the oxygen (Table 4) but deduced the electron transfer to be compensated by a transfer from the protein to the iron. Pauling has suggested a charge separation within the oxygen molecule of one electron [12], i.e. Fe(II)–O^+–O^-, while our calculations predict a significant, but much smaller separation (Table 4).

Support for Weiss' configuration (Fe(III).O_2^-) has been claimed by analogy with the model cobalt complexes [29]. The cobalt oxygen adducts can be represented formally by Co(III).O_2^- because ESR studies have established that the single unpaired electron is mostly associated with the oxygen. However, our calculations show that this does not necessarily infer the corresponding Fe(III).O_2^- in oxyhaemoglobin. The z^2 orbital (unoccupied in oxyhaemoglobin) is thoroughly mixed with the oxygen 2_{p_z} orbital for most metal-oxygen geometries [19]. In the cobalt adducts this z^2 orbital is singly occupied so that unpaired electron character is associated with the oxygen. Specific calculations on some cobalt-oxygen adducts are in progress in our laboratory.

Now, the particular geometry of the iron-oxygen system is of interest. The relative strengths of the iron-oxygen bond can be estimated from the calculated overlap populations [30]. Each atom is assigned a net overlap population, NOP, which is due to that atom's bonding with neighbouring atoms, and we assumed that the system which predicts the largest total NOP for the oxygen molecule, corresponds to the bonding in oxyhaemoglobin. The NOP values are listed in Table 4. Although these NOP values are sensitive to the assumed bond lengths, consistent variation of bond lengths affects the magnitude of the NOP's but not the relative values, and any comparison of bond strengths, as a function of geometry, can only be made for fixed bond distances.

Both asymmetric systems (3 and 5) predict a stronger oxygen binding than the extreme cases (2 and 4), with the Pauling model (system 3) predicting the strongest of all. These conclusions agree well with our earlier results [14] from other models.

The Mössbauer data can be used for an independent prediction of the best simulation. When the plot of Fig. 3 is extrapolated to the observed quadrupole splitting of oxyhaemoglobin, only systems 3 and 5 lie near the line and the Pauling model (3) is the better fit. The asymmetric contribution, η, to the B values is small (0.001 for systems 3 and 5), in agreement with experimental analyses [21], and therefore is not the cause of the unusually large quadrupole splitting in oxyhaemoglobin. We consider this unusual magnitude to be due to covalent effects and the proposed donation of two electrons from the protein.

Conclusion

We have applied a theoretical model to a number of iron porphyrin derivatives and have found a good correlation between theoretical and experimental EFG values. Although the porphyrin ring has been grossly approximated, the consequent errors were constant for all systems studied and the model was appropriate for a discussion of ground state properties of the iron itself. A new description of the ground state in some high-spin iron(III) porphyrins has led to the first correct prediction of a positive EFG, while the proposed two electron transfer to the iron-oxygen system in haemoglobin (or myoglobin) accounts for not only the stability of the oxygen adduct but also the observed sign of the EFG.

Acknowledgements. I wish to thank Prof. J. F. Duncan for many discussions and financial support from U.S.A.F. Grant No. A.F.O.S.R. 1236-69 is gratefully acknowledged.

References

1. Antonini, E.: Physiol. Rev. **45**, 123 (1965).
2. Jug, K.: Theoret. chim. Acta (Berl.) **14**, 91 (1969).
3. Zerner, M., Gouterman, M.: Theoret. chim. Acta (Berl.) **4**, 44 (1966).
4. Hinze, J., Jaffé, H. H.: J. Amer. chem. Soc. **84**, 540 (1962).
5. Wolfsberg, M., Helmholz, L.: J. chem. Physics **20**, 837 (1952).
6. Guzy, C. M., Raynor, J. B., Symons, M. C. R.: J. chem. Soc. A 2299 (1969).
7. Perutz, M. F.: Proc. Roy. Soc. B **173**, 113 (1969).
8. Ohno, K., Tanabe, Y., Susaki, F.: Theoret. chim. Acta (Berl.) **1**, 378 (1963).
9. Slater, J. C.: Physic. Rev. **36**, 57 (1930).
10. Zerner, M., Gouterman, M., Kobayashi, H.: Theoret. chim. Acta (Berl.) **6**, 363 (1966).
11. Bailey, J. P. M.: Report No. CD 2091, DSIR, New Zealand (1967).
12. Pauling, L.: Nature **203**, 182 (1964).
13. Griffith, J. S.: Proc. Roy. Soc. A **235**, 23 (1956).
14. Halton, M. P.: Theoret. chim. Acta (Berl.), in press.
15. Pauling, L., Coryell, C. D.: Proc. Natl. Acad. Sci. **22**, 159 (1936); ibid. **22**, 210 (1936).
16. Gibson, J. F., Ingram, D. J., Schonland, D.: Discuss. Faraday Soc. **26**, 72 (1958).
17. George, P., Beetlestone, J., Griffith, J. S.: Rev. mod. Physics, 441 (1964).
18. Cotton, F. A., Harris, C. G.: Proc. Natl. Acad. Sci. **56**, 12 (1966).
19. Halton, M. P.: Ph. D. Thesis, Victoria University of Wellington, New Zealend (1971).
20. Gonser, U., Grant, R. W.: Biophys. J. **5**, 823 (1965).
21. Lang, G., Marshall, W.: Proc. physic. Soc. **87**, 3 (1966).

22. Weissbluth, M., Maling, J. E.: J. chem. Physics **47**, 4166 (1967).
23. Moss, T. H., Bearden, A. J., Caughey, W. S.: J. chem. Physics **51**, 2624 (1969).
Han, P. S., Das, T. P., Rettig, M. F.: Theoret. chim. Acta (Berl.) **12**, 178 (1968).
24. Kotani, M.: Ann. N.Y. Acad. Sci. **158**, 20 (1969).
25. Blume, M.: Physic. Rev. Letters **14**, 96 (1965).
26. Caughey, W. S., Alben, J. O., Beaudreau, C. A.: In: Oxidases and Related Redox Systems, ed. King, T. E., Mason, H. S., Morrison, M., p. 97. London: Wiley 1964.
27. Caughey, W. S., Eberspaecher, H., Fuchsman, W. H., McCoy, S.: Ann. N.Y. Acad. Sci. **153** (3), 722 (1969). Crumbliss, A. L., Basolo, F.: J. Amer. chem. Soc. **92** (1), 55 (1970).
28. Weiss, J. J.: Nature **202**, 83 (1964).
29. Schrauzer, G. N., Lian Pin Lee: J. Amer. chem. Soc. **92** (6), 1551 (1970).
Walker, F. A.: J. Amer. chem. Soc. **92** (14), 4235 (1970).
Nan-Loh Yang, Oster, G.: J. Amer. chem. Soc. **92** (17), 5265 (1970).
30. Mulliken, R. S.: J. chem. Physics **23**, 1833 (1955).

Dr. M. P. Halton
Chemistry Department
Victoria University of Wellington, New Zealand